Hematopoietic cell-specific knockout Hspa9 impairs natural killer cell function and alters the Akt/mTOR axis in mice

XIAOKANG ZENG[1*], JIEYU ZHANG[2*], CAIYING LIANG[1], JIE YAO[2] and ZUQIANG WU[1]

[1]Laboratory Center, School of Medicine, The Sixth Affiliated Hospital of South China University of Technology (Nanhai District People's Hospital of Foshan), Foshan, Guangdong 528200, P.R. China; [2]Clinical Laboratory, School of Medicine, The Sixth Affiliated Hospital of South China University of Technology (Nanhai District People's Hospital of Foshan), Foshan, Guangdong 528200, P.R. China

Received March 18, 2026; Accepted July 3, 2026

DOI: 10.3892/etm.2026.13249

Abstract. Natural killer (NK) cells are crucial components of the innate immune system, serving vital roles in tumor killing and antiviral immunity. Heat shock protein family A (Hsp70) member 9 (Hspa9), a molecular chaperone localized to the mitochondrial matrix and inner membrane, is essential for maintaining mitochondrial homeostasis. However, its role in regulating NK cells remains unclear. The present study aimed to investigate the impact of the Hspa9 on NK cell regulation and its underlying molecular mechanism. By knocking out Hspa9 at the hematopoietic cell stage, NK cell numbers were found to be markedly reduced in the spleen, bone marrow and liver of mice. Hspa9-deficient NK cells exhibited significantly reduced IFN-γ secretion and CD107a expression. Mechanistically, Hspa9 deficiency led to perturbed expression of surface receptors CD117, CD127 and killer cell lectin-like receptor subfamily A, member 9, which may underlie the observed alteration in maturation status. Furthermore, the impaired NK cell function may be associated with suppressed activation of the Akt/mTOR signaling pathway. In summary, the present study reveals a novel role for Hspa9 in regulating NK cell function, proposes a potential regulatory mechanism and identifies Hspa9 as a promising molecular target for modulating NK cell biology.

Correspondence to: Dr Xiaokang Zeng or Dr Zuqiang Wu, Laboratory Center, School of Medicine, The Sixth Affiliated Hospital of South China University of Technology (Nanhai District People's Hospital of Foshan), 120 Guidan Road, Shishan, Nanhai, Foshan, Guangdong 528200, P.R. China
E-mail: kangki@163.com
E-mail: ywuzq@scut.edu.cn

*Contributed equally

Key words: Hspa9, natural killer cells, natural killer cell function, mTOR/Akt signaling pathway

Introduction

Natural killer (NK) cells are a vital component of the innate immune system and serve as the body's first line of defense against tumors and infections (1). Unlike T and B lymphocytes, NK cells do not require prior antigen sensitization to mount a rapid response, enabling them to recognize and eliminate target cells within hours of encountering a threat. They participate in immune regulation through multiple mechanisms, including the release of cytotoxic granules (perforin and granzymes) that induce apoptosis in malignant or infected cells, secretion of pro-inflammatory cytokines (such as IFN-γ and tumor necrosis factor-α) and chemokines that recruit and activate other immune cells, and dynamic cross-talk with dendritic cells, macrophages and T cells to orchestrate both innate and adaptive immunity (2). The effector functions of NK cells are tightly regulated by a complex network of activating and inhibitory receptors, which integrate extracellular cues to determine the threshold of NK cell activation. In addition to receptor signaling, cellular metabolism has emerged as a critical rheostat for NK cell activity. Key metabolic processes, including glycolysis, mitochondrial oxidative phosphorylation and fatty acid oxidation, can be dynamically modulated to meet the bioenergetic and biosynthetic demands of resting, activated or memory-like NK cells (3). Dysregulation of these metabolic pathways has been associated with impaired NK cell function in various disease settings, including cancer and chronic viral infections.

The development of NK cells from hematopoietic stem cells in the bone marrow proceeds through a series of well-defined stages, including the common lymphoid progenitor, the NK progenitor and the immature NK cell, followed by their subsequent maturation in peripheral tissues such as the spleen, liver and lymph nodes (4). This entire process is orchestrated by a delicate balance of transcription factors, including eomesdermin, T-box expressed in T cells, inhibitor of DNA binding 2 and GATA binding protein 3, which act in a stage-specific manner to control lineage commitment, survival and functional maturation (5,6). In parallel, cytokine signals, primarily IL-15 but also IL-12, IL-18 and type I interferons, provide essential survival and proliferation cues through receptor complexes that activate downstream JAK-STAT and PI3K-Akt pathways (7). Moreover, intrinsic metabolic checkpoints, such

as the balance between glycolysis and oxidative phosphorylation, as well as mitochondrial fitness, have recently been recognized as key determinants that shape NK cell development and homeostasis (8).

Simultaneously, the effector functions of mature NK cells, including direct cytotoxicity via perforin/granzyme release and cytokine production are tightly controlled by a highly integrated network of activating receptors and inhibitory receptors that recognize self-major histocompatibility class (MHC) class I molecules (9). The integration of opposing signals from these receptors determines the threshold for NK cell activation. In addition, intracellular signaling cascades, including the PI3K-Akt-mTOR axis, the MAPK/ERK pathway and JAK-STAT pathways, coordinate cytoskeletal reorganization, granule polarization and transcriptional reprogramming required for effective target cell elimination. Furthermore, epigenetic modifications, such as DNA methylation, histone acetylation and methylation, as well as non-coding RNAs, have emerged as critical regulators that fine-tune the expression of receptors and effector molecules during NK cell education, licensing and memory-like differentiation (10).

Glucose-regulated protein 75 [GRP75; also known as Heat shock protein family A (Hsp70) member 9 (Hspa9)] functions as a critical tether at mitochondria-associated membranes. It physically interacts with the endoplasmic reticulum calcium release channel inositol 1,4,5-trisphosphate receptor type 1 (IP3R1) and the mitochondrial outer membrane protein voltage-dependent anion-selective channel 1 (VDAC1), facilitating ER-mitochondria contact and efficient calcium transfer into the mitochondria (11). However, dysregulation of this IP3R1/GRP75/VDAC1 axis, resulting in excessive mitochondrial calcium influx, can trigger calcium overload, mitochondrial dysfunction and subsequent cellular apoptosis, as observed in conditions such as skeletal muscle atrophy (12). This highlights the delicate balance maintained by Hspa9 in cellular physiology.

While the role of Hspa9 in mitochondrial homeostasis is established, its specific function in NK cells remains largely unexplored. The present study aimed to investigate the role of Hspa9 in the development and functional regulation of NK cells, as well as its modulatory effect on the PI3K-Akt signaling pathway, a key pathway in NK cells. The aim was to elucidate the regulatory function and molecular mechanism of Hspa9 in NK cells. The present findings will broaden the theoretical understanding of NK cell functional regulation.

Materials and methods

Mice. $Hspa9^{flox/flox}$ mice (stock no. S-CKO-02995) and $\beta 2m^{-/-}$ mice (stock no. KOCMP-12010-B2m-B6J-VA) were imported from Cyagen Biosciences, Inc. $Hspa9^{flox/flox}$ mice were crossed with Vav1-cre mice (B6/Vav1-cre; stock no. C001019; Cyagen Biosciences, Inc.) to obtain hematopoietic cell-specific Hspa9-knockout mice. The experiments were conducted using paired 8-week-old male or female C57BL/6 mice (18-22 g; n=80). Mice were divided into two groups (40 mice/group): i) Wild-type group ($Hspa9^{fl/fl}$ mice); and ii) Hspa9 conditional knockout group ($Hspa9^{fl/fl}$ Vav-cre mice). Animals were housed in an SPF facility at 22±2˚C, 50-60% humidity, with a 12-h light/dark cycle. They were housed group-housed, ≤5 per cage with ample bedding, nesting material and environmental enrichment (tunnels and wooden blocks). Standard chow and autoclaved water were available *ad libitum*. Soft diet or gel was provided for debilitated animals to facilitate feeding and prevent excessive weight loss. During the experiment, all animals were clinically observed at least once daily. Body weight was measured every 3 days and recorded in detail. The humane endpoints for mice in the present study were established as a body weight loss of >20% of the initial weight, or the manifestation of severe clinical signs such as hunched posture, ruffled fur, lethargy, reduced response to external stimuli, respiratory distress or persistent diarrhea. For all mice except those with B16 melanoma lung metastasis, animals were anesthetized with tribromoethanol (125 mg/kg) by intraperitoneal injection. Subsequently, they were euthanized by cervical dislocation and dissected to collect the spleen, liver, lungs, and other organs or tissues for further experiments (13). At the end of the experiment in mice with B16 melanoma lung metastasis, the mice were euthanized in a 10-liter chamber with a gradual CO_2 inflow at a rate of 3 l/min, which corresponds to a volume displacement rate of 30% per min. The animal experiment protocols were reviewed and approved by the Animal Ethics Committee of the Sixth Affiliated Hospital of South China University of Technology (Nanhai District People's Hospital of Foshan; Foshan, China; approval no. ZXSY-JY-ZXK-250918-002). The animal experiments were implemented in strict accordance with the approved protocols. We followed the methods of Zeng *et al* (14).

Analysis of Hspa9 expression across immune cell types in mice using public databases. Data on the RNA expression of Hspa9 in different mouse cell types were obtained from the Expression Atlas database (https://www.ebi.ac.uk/gxa/home) and the expression levels were compared among the cell types.

Antibodies and flow cytometry. The methods were performed as previously described by Zeng *et al* (14). The surface and functional markers of the immune cells were detected using a flow cytometer from BD Biosciences (CANTO II). Fluorescein-labeled monoclonal antibodies against mouse CD3e, NK1.1, CD11b, CD27, CD98, CD71, CD69, CD25, killer cell lectin-like receptor subfamily G member 1 (KLRG1), IFN-γ, CD107a, CD127, Ly49A, Ly49G2, NKp46, Ly49C/I, CD117, NKG2A, 2B4, NKG2D and an isotype control were purchased from Thermo Fisher Scientific, Inc. (Table SI). To analyze protein expression on cell surfaces, the mononuclear cells of spleen from the mice were obtained. A 70-μm cell strainer (Wuxi NEST Biotechnology Co., Ltd.) was placed in a 35-mm cell culture dish (Corning, Inc.) containing 2 ml RPMI 1640 medium (Gibco; Thermo Fisher Scientific, Inc.). The freshly isolated mouse spleen was placed onto the strainer and gently mashed with the plunger of a 2.5-ml syringe until the tissue passed through the mesh to generate a single-cell suspension. The suspension was transferred to a 15-ml centrifuge tube (Corning, Inc.) and centrifuged at 400 x g for 5 min at 4˚C. The supernatant was discarded, and the cell pellet was resuspended in 1 ml of red blood cell lysis buffer (MedChemExpress) by gentle pipetting. After thorough mixing, the tube was incubated on ice for 5 min. Next, 5 ml phosphate-buffered saline (PBS) (Sangon Biotech Co., Ltd.)

was added, and the cells were centrifuged again at 400 x g for 5 min at 4˚C. The supernatant was removed, and the pellet was resuspended in 1 ml PBS containing 1% fetal bovine serum (FBS) (Gibco; Thermo Fisher Scientific, Inc.). Finally, the cell suspension was filtered through a new 70-μm cell strainer to obtain the mononuclear cell suspension. The mononuclear cells ($1x10^6$) were stained with the specific antibodies dissolved in 100 μl PBS containing 2% FBS. Cells were washed once with PBS and analyzed using the flow cytometer. For the detection of intracellular proteins, such as Hspa9, lymphocytes were fixed with Phosflow Lyse/Fix buffer and permeabilized with Phosflow Perm buffer III (Invitrogen; Thermo Fisher Scientific, Inc.; cat. no. 88-8824-00) prior to staining with antibodies. For Hspa9, Akt, phosphorylated (p-)Akt and mTOR staining, after the primary antibody staining was completed, samples were washed with PBS and secondary antibody (goat anti-Rabbit IgG-PE) was added for staining. The fluorescence signal was detected using flow cytometry. The data were analyzed using FlowJo™ software (v10.4; FlowJo, LLC; BD Biosciences). The mean fluorescence intensity (MFI) was defined as the MFI of the gated cell population, which is less sensitive to outliers and therefore suitable for skewed fluorescence distributions.

Detection of CD107a expression and intracellular staining of NK cells. The methods of Zeng *et al* (14) and Liang *et al* (15) were followed. CD107a is a lysosomal membrane protein. During the degranulation process, the cell membrane combines with the lysosome. Therefore, the expression level of CD107a is related to cell degranulation. First, to activate NK cells in the mice, the mice were intraperitoneally injected with 200 μg Poly I:C (cat. no. P9582; MilliporeSigma) for NK cell activation. After 18 h, the spleen was removed and the splenocytes were processed to obtain splenic mononuclear cells, as aforementioned. The splenocytes ($2x10^6$ cells) were stained with CD107a antibody and co-cultured with Yac-1 cells (cat. no. TIB-160; ATCC) ($2x10^6$ cells) for 1 h in DMEM (cat. no. 11885084; Gibco; Thermo Fisher Scientific, Inc.) with 10% FBS (cat. no. 10099141; Gibco; Thermo Fisher Scientific, Inc.) in a culture incubator (37˚C, 5% CO_2). Next, a Golgi inhibitor (GolgiStop™; BD Biosciences) was added to prevent the release of intracellular proteins. Cells were cultured for a further 4 h. The cells were collected for extracellular staining (Nkp46). A total of 250 μl Fixation/Permeabilization solution (cat. no. 00-5523-00; Thermo Fisher Scientific, Inc.) was added, and the cells were permeabilized at 4˚C for 20 min protected from light. The samples were washed twice with 1 ml cytoperm/wash buffer (cat. no. 00-5523-00; Thermo Fisher Scientific, Inc.). Specific intracellular staining antibodies for IFN-γ were added and the samples incubated at room temperature for 30 min protected from light. The cells were washed twice with 1 ml cytoperm/wash buffer, then the resuspended cells were analyzed using the flow cytometer. The data were analyzed using FlowJo™ software (v10.4; FlowJo, LLC; BD Biosciences).

In vivo β2M$^{-/-}$ cell clearance assay. β2m$^{-/-}$ mice (stock no. KOCMP-12010-B2m-B6J-VA) were imported from Cyagen Biosciences, Inc. The experiments were conducted using 8-week-old male C57BL/6 mice (18-22 g; n=3). Animals were housed in an SPF facility at 22±2˚C and 50-60% humidity, with a 12-h light/dark cycle. The mice were group-housed, with ≤5 animals per cage, with ample bedding, nesting material and environmental enrichment (tunnels and wooden blocks). Standard chow and autoclaved water were available *ad libitum*. Splenocytes from wild-type and β2M$^{-/-}$ mice were labeled with 5 μM Carboxyfluorescein Diacetate Succinimidyl Ester (cat. no. 21888; MilliporeSigma) and 5 μg/ml Cell Tracker™ Violet (CTV) (cat. no. C34557; Thermo Fisher Scientific, Inc.), respectively. The splenocytes from wild-type and β2M$^{-/-}$ mice were then intravenously injected at 1:1 ratio ($1x10^6$) into the Hspa9$^{fl/fl}$ and Hspa9$^{fl/fl}$ Vav-cre mice which were pretreated with poly I:C 18 h before. After 6 h, the proportion of CTV-positive β2M$^{-/-}$ cells in the spleens and lymph nodes of the recipient mice was quantified using flow cytometry (CANTO II; BD Biosciences). The data were analyzed using FlowJo™ software (v10.4; FlowJo, LLC; BD Biosciences).

Detection of mitochondrial mass. The splenocytes from Hspa9$^{fl/fl}$ and Hspa9$^{fl/fl}$ Vav-cre mice were cultured in RPMI 1640 medium containing recombinant human IL-2 (1,000 IU/ml) (cat. no. 200-02-50UG; Thermo Fisher Scientific, Inc.) for 4 h. For the detection the mitochondrial mass, NK cells were stained with surface markers CD3 and NK1.1 before being stained with the dye MitoTracker Green FM (Sigma-Aldrich; Merck KGaA; cat. no. M7514) for 30 min at room temperature. MitoTracker Green FM in CD3$^-$ NK1.1$^+$ cells was detected using flow cytometry (CANTO II; BD Biosciences). MFI of MitoTracker Green FM was used to measure the mitochondrial mass. The data were analyzed using FlowJo™ software (v10.4; FlowJo, LLC; BD Biosciences).

Detection of reactive oxygen species (ROS) generation. Splenocytes were cultured in RPMI 1640 medium containing recombinant human IL-2 (1,000 IU/ml) for 4 h. Rotenone (MedChemExpress; cat. no. HY-B1756) was used to induce ROS at a concentration of 1 μM for 1 h. For the detection of ROS generation, NK cells were stained with surface markers CD3 and NK1.1 before being stained with the dye 2',7'-dichlorofuorescin diacetate (DCFH-DA; Sigma-Aldrich; Merck KGaA; cat. no. D6883) for 30 min at room temperature. DCFH-DA in CD3$^-$ NK1.1$^+$ cells was detected using flow cytometry (CANTO II; BD Biosciences). The data were analyzed using FlowJo™ software (v10.4; FlowJo, LLC; BD Biosciences). MFI of DCFH-DA was used to assess the ROS levels.

B16 melanoma lung metastasis mouse model. B16-F10 melanoma cells (cat no. CRL-6475; ATCC) were cultured in DMEM (catalog no. 11885084; Gibco; Thermo Fisher Scientific, Inc.) with 10% FBS (cat. no. 10099141; Gibco; Thermo Fisher Scientific, Inc.) in a culture incubator (37˚C, 5% CO_2). Logarithmic-phase cells were suspended in 1X HBSS and intravenously injected into mice ($3x10^5$ cells/mouse) as previously described by He *et al* (16). After 14 days, the mice were sacrificed by CO_2 inhalation as aforementioned. The lungs were weighed, and the number of lung surface nodules was counted under a dissecting microscope.

Statistical analysis. GraphPad Prism 7 software (Dotmatics) was used to plot the graphs. Unpaired Student's t-tests

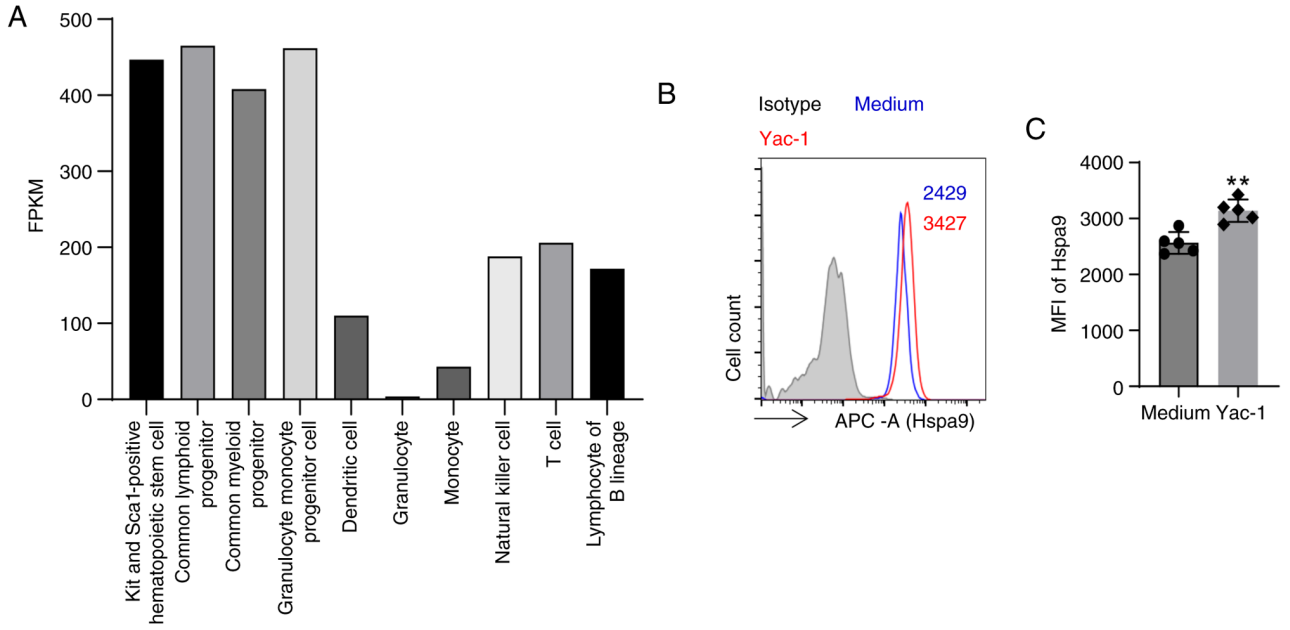

Figure 1. Hspa9 is highly expressed in hematopoietic cells, and its expression in NK cells increases upon Yac-1 cell stimulation. (A) Analysis of Hspa9 RNA levels across mouse hematopoietic stem cells and immune cell types using the Expression Atlas database. (B) Flow cytometry analysis of Hspa9 expression on mouse splenic NK cells with or without Yac-1 cell stimulation for 4 h. (C) Statistical graph of Hspa9 expression on mouse splenic NK cells with or without Yac-1 cell stimulation for 4 h. Data are shown as mean ± SD. Unpaired Student's t-tests (two-tailed) were performed using Prism software. **P<0.01. Hspa9, Heat shock protein family A (Hsp70) member 9; NK, natural killer; MFI mean fluorescence intensity; FPKM, fragments per kilobase million.

(two-tailed) were performed using GraphPad Prism 7. Dunnett's post hoc tests were performed based on the ANOVA for multivariate data analysis using SPSS 22.0 (IBM Corp.). P<0.05 was considered to indicate a statistically significant difference.

Results

Hspa9 is highly expressed in NK cells, and its expression increases upon tumor cell stimulation. Analysis of public databases revealed that Hspa9 is highly expressed in mouse common lymphoid progenitors (CLPs), kit and SCA1-positive hematopoietic stem cell, lymphoid progenitor, myeloid progenitor, monocyte progenitor within the immune system, with high levels also observed in NK, T and B cells (Fig. 1A). Yac-1 cells are target cells for NK cells. Yac-1 cells continuously secrete IL-10, leading to extremely low expression of MHC-I molecules on their surface. The lack of MHC-I molecules prevents effective binding of inhibitory receptors on NK cells, resulting in sustained activation of NK cells. To investigate the relationship between Hspa9 expression and NK cell activation, Hspa9 expression was examined in mouse NK cells following stimulation with the NK-sensitive target cell line Yac-1 for 4 h. Experimental validation confirmed that Yac-1 stimulation significantly elevated Hspa9 protein levels in mouse NK cells (Fig. 1B). Stimulation with Yac-1 cells increases the expression of Hspa9, suggesting that Hspa9 may be involved in the regulation of NK cell activation.

Conditional knockout of Hspa9 in mouse hematopoietic cells reduces NK cell numbers in the spleen, bone marrow and liver. To investigate the role of hematopoietic Hspa9 in NK cells, Hspa9$^{fl/fl}$ Vav-cre mice were utilized and NK cell populations were analyzed across various tissues. First, the knockout efficiency of Hspa9 in splenic NK cells from Hspa9$^{fl/fl}$ Vav-cre mice was examined and demonstrated that Hspa9 was barely detectable in these cells, indicating that Hspa9 was successfully knocked out in NK cells of Hspa9$^{fl/fl}$ Vav-cre mice (Fig. 2A and B). Next, the phenotype of NK cells in Hspa9$^{fl/fl}$ Vav-cre mice was assessed. The gating strategy for flow cytometry is shown in Fig. S1. Results showed a significant reduction in NK cell numbers in the spleen, bone marrow and liver of Hspa9$^{fl/fl}$ Vav-cre mice compared with Hspa9$^{fl/fl}$ controls (Fig. 2C-E), indicating that Hspa9 expression in the hematopoietic cell is crucial for NK cell homeostasis.

Hspa9 deficiency in hematopoietic cells of mice may impair NK cell maturation. To further assess the impact of hematopoietic Hspa9 deletion on NK cell development, maturation stages were analyzed using flow cytometry. In both the spleen and bone marrow of Hspa9$^{fl/fl}$ Vav-cre mice, the proportion and absolute number of terminally mature CD11b^{+} NK cells was significantly decreased, while the proportion and absolute number of early mature CD27^{+}CD11b^{+} NK cells was markedly increased compared to Hspa9$^{fl/fl}$ controls (Fig. 3A-D). Consistent findings were obtained using an alternative marker set: The frequency of NK cell precursors (NKp) was significantly elevated, whereas the proportion and absolute number of mature NK cells was reduced in Hspa9$^{fl/fl}$ Vav-Cre mice compared to Hspa9$^{fl/fl}$ controls (Fig. 3E-H). These results demonstrate that Hspa9 deficiency may disrupt NK cell maturation.

Conditional knockout of Hspa9 in hematopoietic cells of mice disrupts the expression of NK cell surface receptors. To explore the mechanism underlying the maturation blockade, the expression of key surface receptors on NK cells from

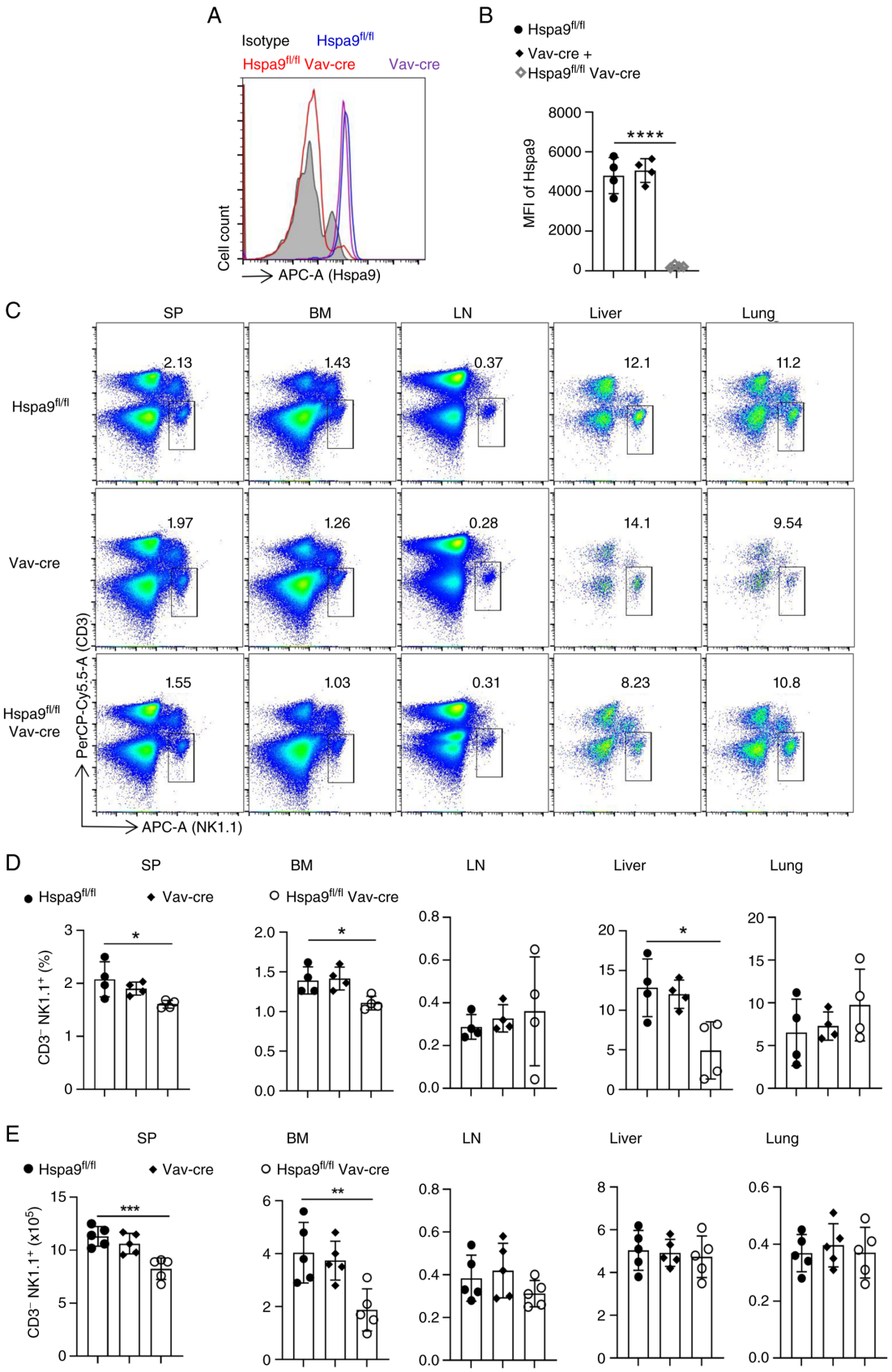

Figure 2. Conditional knockout of Hspa9 in mouse hematopoietic cells reduces NK cell numbers in the spleen, bone marrow, and liver. (A) Representative flow cytometry plot showing Hspa9 expression in splenic NK cells from Hspa9$^{fl/fl}$, Vav-cre, and Hspa9$^{fl/fl}$ Vav-cre mice. (B) Statistical graph of Hspa9 expression in splenic NK cells from Hspa9$^{fl/fl}$, Vav-cre, and Hspa9$^{fl/fl}$ Vav-cre mice. (C) Representative flow cytometry plots of NK cells in SP, BM, LN, liver and lung from Hspa9$^{fl/fl}$, Vav-cre, and Hspa9$^{fl/fl}$ Vav-cre mice. (D) Statistical graphs showing the proportion of NK cells in SP, BM, LN, liver and lung from Hspa9$^{fl/fl}$, Vav-cre, and Hspa9$^{fl/fl}$ Vav-cre mice. (E) Statistical graphs showing the absolute number of NK cells in SP, BM, LN, liver and lung from Hspa9$^{fl/fl}$, Vav-cre, and Hspa9$^{fl/fl}$ Vav-cre mice. Data are shown as mean ± SD. One-way ANOVA with Dunnett's post hoc tests was performed using SPSS 22.0. *P<0.05, **P<0.01, ***P<0.001, ****P<0.0001. Hspa9, Heat shock protein family A (Hsp70) member 9; NK, natural killer; SP, spleen; BM, bone marrow; LN, lymph nodes; MFI mean fluorescence intensity.

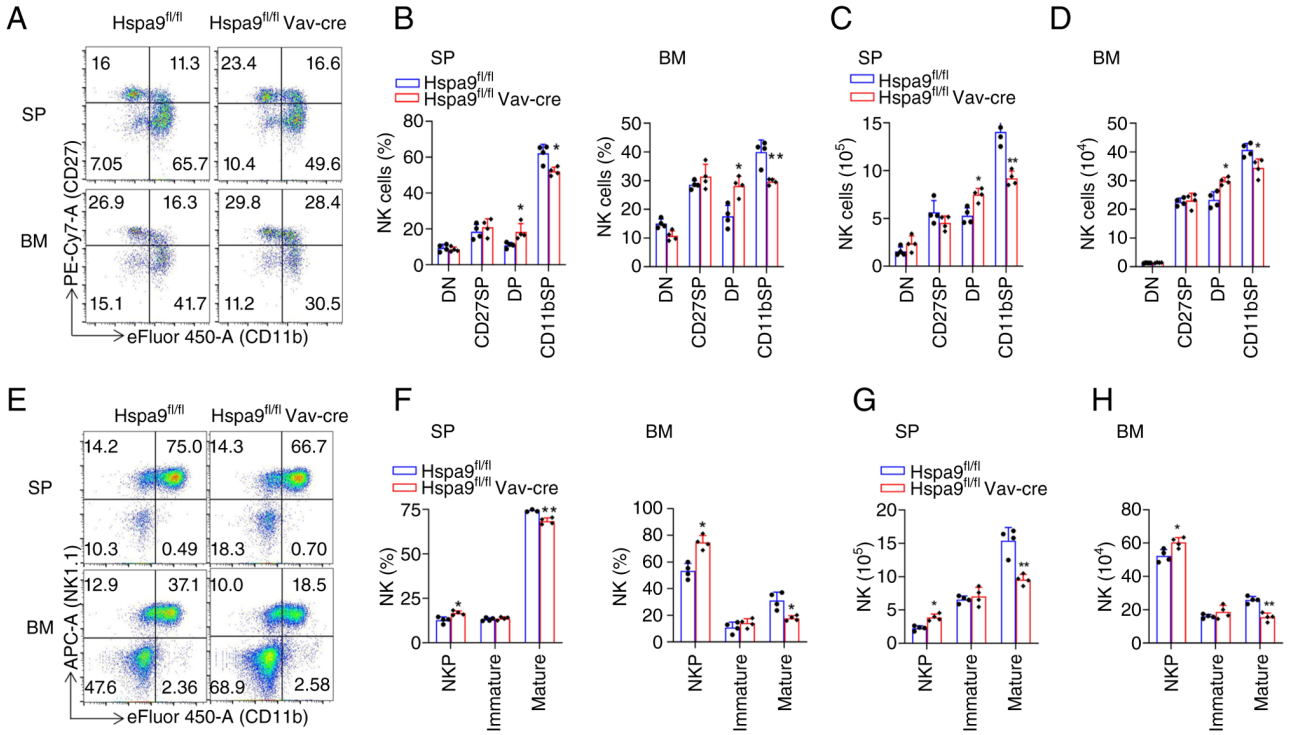

Figure 3. Conditional knockout of Hspa9 in mouse hematopoietic cells may impair NK cell maturation. (A) Representative flow cytometry plots delineating mouse NK cell developmental stages using CD27 and CD11b markers in SP and BM from Hspa9$^{fl/fl}$ and Hspa9$^{fl/fl}$ Vav-cre mice. (B) Statistical graphs showing the proportion of NK cells at different developmental stages in SP and BM from Hspa9$^{fl/fl}$ and Hspa9$^{fl/fl}$ Vav-cre mice. Statistical graphs showing the absolute number of NK cells at different developmental stages in the (C) SP and (D) BM from Hspa9$^{fl/fl}$ and Hspa9$^{fl/fl}$ Vav-cre mice. (E) Representative flow cytometry plots delineating mouse NK cell developmental stages using NK1.1 and CD11b markers in SP and BM from Hspa9$^{fl/fl}$ and Hspa9$^{fl/fl}$ Vav-cre mice. (F) Statistical graphs showing the proportion of NK cells at different developmental stages in SP and BM from Hspa9$^{fl/fl}$ and Hspa9$^{fl/fl}$ Vav-cre mice. Statistical graphs showing the absolute number of NK cells at different developmental stages in the (G) SP and (H) BM from Hspa9$^{fl/fl}$ and Hspa9$^{fl/fl}$ Vav-cre mice. Data are shown as mean ± SD. Unpaired Student's t-tests (two-tailed) were performed using Prism software. *P<0.05, **P<0.01. Hspa9, Heat shock protein family A (Hsp70) member 9; NK, natural killer; SP, spleen; BM, bone marrow; DN, double negative NK cells (CD27^{-}CD11b^{-}); CD27SP, single-positive NK cells (CD27^{+}CD11b^{-}); DP, double-positive NK cells (CD27^{+}CD11b^{+}); CD11bSP, single-positive NK cells (CD27^{-}CD11b^{-}); NKP, double-negative NK cells (NK1.1^{-}CD11b^{-}); immature, single-positive NK cells (NK1.1^{+}CD11b^{-}); mature, double-positive NK cells (NK1.1^{+}CD11b^{+}).

Hspa9$^{fl/fl}$ Vav-Cre mice was analyzed. In splenic NK cells, expression of CD117 and CD127 was significantly upregulated, while expression of Ly49C/I and Ly49D was downregulated on NK cells from Hspa9$^{fl/fl}$ Vav-Cre mice (Fig. 4A and B). In bone marrow NK cells, CD117 expression was increased, whereas Ly49C/I and KLRG1 expression was decreased in Hspa9$^{fl/fl}$ Vav-Cre mice (Fig. 4C and D). These findings suggest that Hspa9 deficiency perturbs NK cell development and altering the expression of critical surface molecules such as CD117, CD127 and Ly49C/I.

NK cells from hematopoietic cell-specific Hspa9-knockout mice exhibit impaired effector functions and antitumor function of Hspa9$^{fl/fl}$ Vav-cre mice is reduced. The function of NK cells from Hspa9$^{fl/fl}$ Vav-Cre mice was evaluated. Upon Yac-1 stimulation, Hspa9-deficient NK cells produced significantly less IFN-γ (Fig. 5A and B) and exhibited reduced CD107a expression compared with wild-type NK cells (Fig. 5C and D). These data indicate that Hspa9 deficiency in the hematopoietic cell may compromise NK cell IFN-γ and degranulation function. Furthermore, Hspa9$^{fl/fl}$ Vav-cre mice showed a diminished ability to clear β2M$^{-/-}$ target cells (Fig. 5E and F) and developed significantly more lung metastases in a B16-F10 melanoma model (Fig. 5G and H). This indicates that the antitumor function of Hspa9$^{fl/fl}$ Vav-cre mice is reduced.

Conditional knockout of Hspa9 in hematopoietic cells suppresses Akt/mTOR signaling in NK cells of mice. To elucidate the molecular mechanism, key signaling pathways which regulate NK cell function were examined. Compared with Hspa9$^{fl/fl}$ mice, NK cells from Hspa9$^{fl/fl}$ Vav-cre mice exhibited significantly decreased mitochondrial mass and significantly increased ROS production (Fig. 6A-D). Flow cytometry analysis revealed that Hspa9-deficient NK cells the activation of the Akt/mTOR pathway was suppressed, as evidenced by reduced phosphorylation of Akt and decreased mTOR expression (Fig. 6E-K). This indicates that in mice with hematopoietic cell-specific knockout of Hspa9, NK cell function is impaired, and the Akt/mTOR signaling pathway in NK cells is also inhibited.

Discussion

Hspa9 is a highly conserved molecular chaperone primarily localized to the mitochondrial matrix and inner membrane. It serves a central role in maintaining mitochondrial homeostasis, participating in processes such as mitochondrial protein import, assembly of oxidative phosphorylation complexes and stabilization of mitochondrial DNA. Beyond its mitochondrial functions, cytosolic Hspa9 can interact with various signaling proteins, influencing pathways related to cell proliferation,

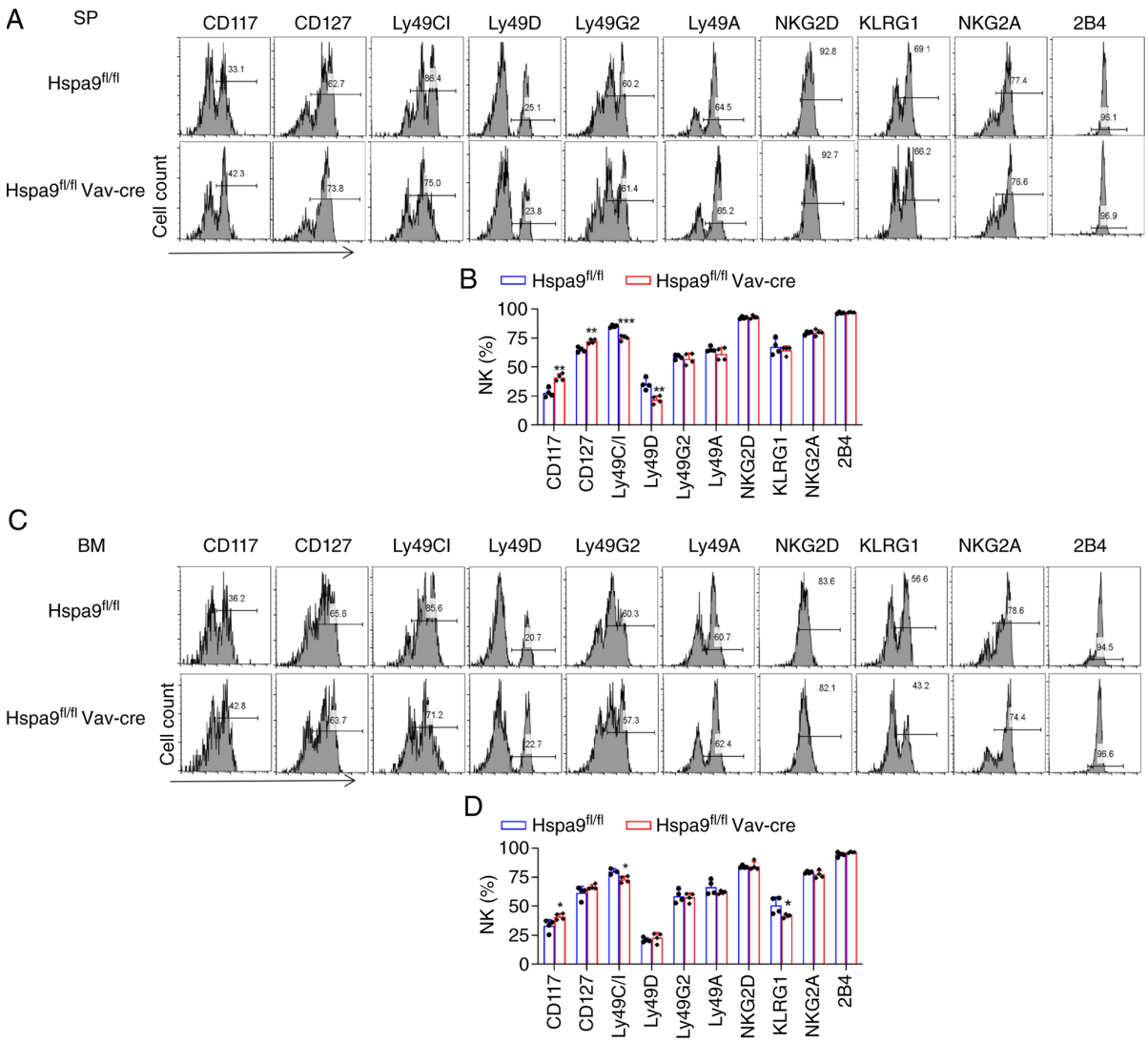

Figure 4. Hematopoietic cell-specific knockout of Hspa9 in mice disrupts NK cell surface receptor expression. (A) Representative flow cytometry plots of surface receptor expression on splenic NK cells from Hspa9$^{fl/fl}$ and Hspa9$^{fl/fl}$ Vav-cre mice. (B) Statistical graph of surface receptor expression on splenic NK cells from Hspa9$^{fl/fl}$ and Hspa9$^{fl/fl}$ Vav-cre mice. (C) Representative flow cytometry plots of surface receptor expression on BM NK cells from Hspa9$^{fl/fl}$ and Hspa9$^{fl/fl}$ Vav-cre mice. (D) Statistical graph of surface receptor expression on BM NK cells from Hspa9$^{fl/fl}$ and Hspa9$^{fl/fl}$ Vav-cre mice. Data are shown as mean ± SD. Unpaired Student's t-tests (two-tailed) were performed using Prism software. *P<0.05, **P<0.01, ***P<0.001. Hspa9, Heat shock protein family A (Hsp70) member 9; NK, natural killer; SP, spleen; BM, bone marrow.

migration and apoptosis (17,18). Notably, elevated Hspa9 expression is frequently observed in multiple solid tumors, including breast cancer, hepatocellular carcinoma and glioma, and is associated with poor patient prognosis (19,20). However, its regulatory role within the immune system remains less explored.

The present study identified a novel function for Hspa9 in NK cell biology. Hspa9 was found to be highly expressed in CLPs and mature NK cells. Furthermore, its protein levels in NK cells increased upon stimulation with tumor target cells (Yac-1), suggesting a potential link between Hspa9 expression and NK cell activation. Using a hematopoietic-specific knockout mouse model (Hspa9$^{fl/fl}$ Vav-cre), Hspa9 was demonstrated to be essential for NK cell homeostasis, as evidenced by a significant reduction in NK cell numbers in the spleen, bone marrow and liver of Hspa9$^{fl/fl}$ Vav-cre mice. This finding is consistent with a prior report implicating Hspa9 as a critical regulator for thymocyte development (21). However, the Hspa9$^{fl/fl}$ Vav-cre mice used mediate gene knockout in hematopoietic cells and all hematopoietic-derived cells, including T cells, B cells, myeloid cells and NK cells. Therefore, although changes were observed in the number, phenotype or function of NK cells in this mouse model, these alterations may not reflect the intrinsic role of Hspa9 in NK cells. In future studies, the use of NK cell-specific knockout mice combined with adoptive transfer experiments will help further clarify the cell-intrinsic function of Hspa9 in NK cells.

Further analysis revealed that mice with Hspa9 deficiency in hematopoietic cells exhibit altered NK cell maturation status. A marked decrease was observed in the proportion of terminally mature CD11b^{+} NK cells alongside an accumulation of earlier developmental intermediates. This maturation block may be associated with dysregulated expression of surface receptors, such as CD117, CD127 and Ly49C/I, in Hspa9-deficient NK cells. The crucial role of Hspa9 in cellular differentiation and

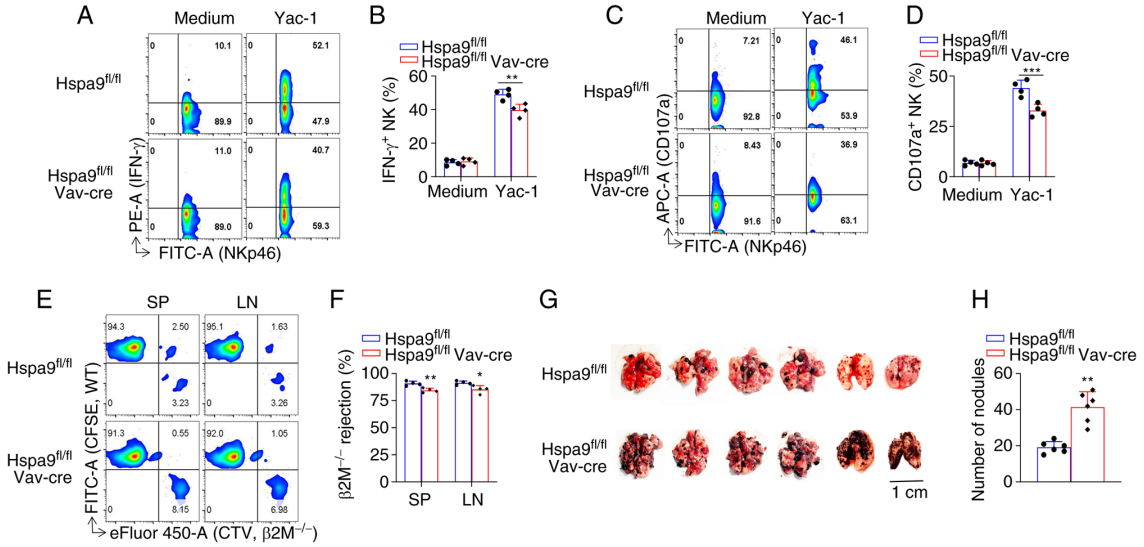

Figure 5. Hematopoietic cell-specific knockout of the mouse Hspa9 gene impairs NK cell function. (A) Representative flow cytometry plots detecting IFN-γ secretion by splenic NK cells from Hspa9$^{fl/fl}$ and Hspa9$^{fl/fl}$ Vav-cre mice. (B) Statistical graph of IFN-γ secretion by splenic NK cells from Hspa9$^{fl/fl}$ and Hspa9$^{fl/fl}$ Vav-cre mice. (C) Representative flow cytometry plots detecting CD107a expression on splenic NK cells from Hspa9$^{fl/fl}$ and Hspa9$^{fl/fl}$ Vav-cre mice. (D) Statistical graph of CD107a expression on splenic NK cells from Hspa9$^{fl/fl}$ and Hspa9$^{fl/fl}$ Vav-cre mice. (E) Representative flow cytometry plots detecting residual β2M$^{-/-}$ cells in the SP and LN of Hspa9$^{fl/fl}$ and Hspa9$^{fl/fl}$ Vav-cre mice at 6 h after cell injection. CFSE is a live-cell fluorescent labeling dye used to label wild-type cells. (F) Statistical graph showing the residual amount of β2M$^{-/-}$ cells in SP and LN from Hspa9$^{fl/fl}$ and Hspa9$^{fl/fl}$ Vav-cre mice at 6 h after cell injection. (G) Representative images of the melanoma lung metastasis in Hspa9$^{fl/fl}$ and Hspa9$^{fl/fl}$ Vav-cre mice. Scale bar, 1cm. (H) Statistical graph of lung metastatic nodule counts in Hspa9$^{fl/fl}$ and Hspa9$^{fl/fl}$ Vav-cre mice. Data are shown as mean ± SD. Unpaired Student's t-tests (two-tailed) were performed using Prism software or one-way ANOVA with Dunnett's post hoc test were performed using SPSS 22.0. *P<0.05, **P<0.01, ***P<0.001. Hspa9, Heat shock protein family A (Hsp70) member 9; NK, natural killer; SP, spleen; BM, bone marrow; LN, lymph nodes; CFSE, 5(6)-carboxyfluorescein diacetate N-succinimidyl ester.

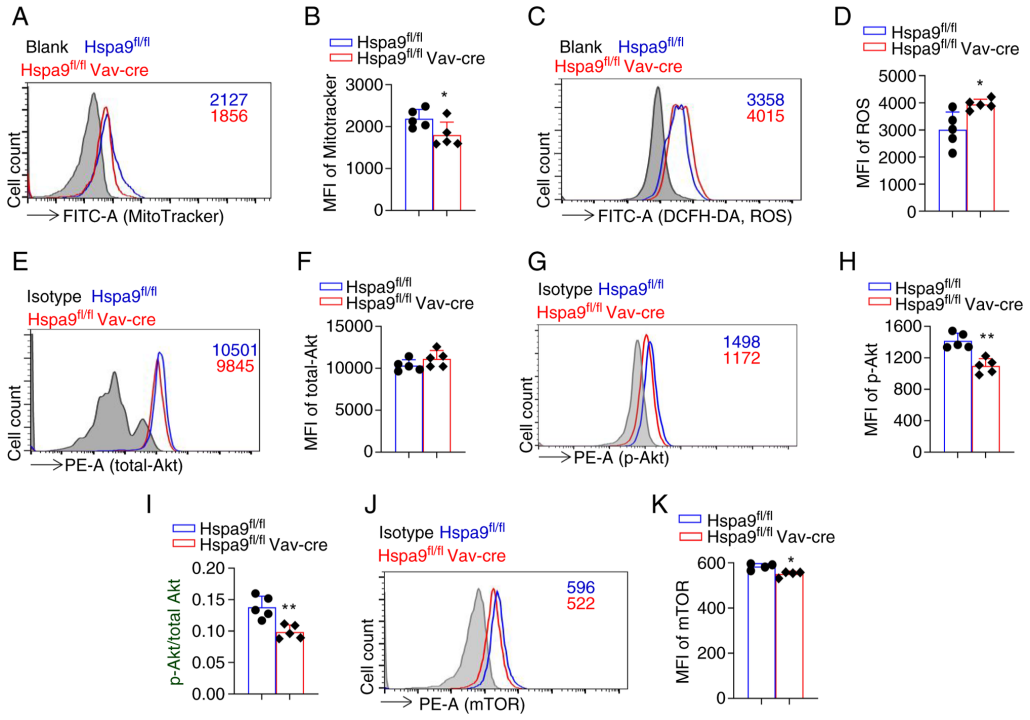

Figure 6. Hematopoietic cell-specific knockout of the mouse Hspa9 gene suppresses Akt/mTOR signaling in NK cells. (A) Representative flow cytometry plot of MitoTracker staining on splenic NK cells from Hspa9$^{fl/fl}$ and Hspa9$^{fl/fl}$ Vav-cre mice. (B) Statistical graph of MFI of MitoTracker on splenic NK cells from Hspa9$^{fl/fl}$ and Hspa9$^{fl/fl}$ Vav-cre mice. (C) Representative flow cytometry plot of ROS staining on splenic NK cells from Hspa9$^{fl/fl}$ and Hspa9$^{fl/fl}$ Vav-cre mice after 1 μM rotenone treatment for 1 h. (D) Statistical graph of MFI of ROS on splenic NK cells from Hspa9$^{fl/fl}$ and Hspa9$^{fl/fl}$ Vav-cre mice after 1 μM rotenone treatment. (E) Representative flow cytometry plot of total-Akt expression on splenic NK cells from Hspa9$^{fl/fl}$ and Hspa9$^{fl/fl}$ Vav-cre mice. (F) Statistical graph of total-Akt expression on splenic NK cells from Hspa9$^{fl/fl}$ and Hspa9$^{fl/fl}$ Vav-cre mice. (G) Representative flow cytometry plot of p-Akt expression on splenic NK cells from Hspa9$^{fl/fl}$ and Hspa9$^{fl/fl}$ Vav-cre mice. (H) Statistical graph of p-Akt expression on splenic NK cells from Hspa9$^{fl/fl}$ and Hspa9$^{fl/fl}$ Vav-cre mice. (I) Statistical graph of the ratio of p-Akt to total Akt on splenic NK cells from Hspa9$^{fl/fl}$ and Hspa9$^{fl/fl}$ Vav-cre mice. (J) Representative flow cytometry plot of mTOR expression on splenic NK cells from Hspa9$^{fl/fl}$ and Hspa9$^{fl/fl}$ Vav-cre mice. (K) Statistical graph of mTOR expression on splenic NK cells from Hspa9$^{fl/fl}$ and Hspa9$^{fl/fl}$ Vav-cre mice. Data are shown as mean ± SD. Unpaired Student's t-tests (two-tailed) were performed using Prism software. *P<0.05, **P<0.01. Hspa9, Heat shock protein family A (Hsp70) member 9; NK, natural killer; MFI, mean fluorescence intensity; p-, phosphorylated; ROS, reactive oxygen species.

survival is supported by studies in other models. For instance, Hspa9 deficiency in zebrafish leads to increased apoptosis and defective hematopoiesis (22), while Hspa9 deficiency disrupting its function can impair energy metabolism and differentiation in neurons (23,24).

Functionally, NK cells from Hspa9$^{fl/fl}$ Vav-cre mice exhibited impaired function. Their ability to secrete IFN-γ and express CD107a was significantly compromised. Although the ability of Hspa9$^{fl/fl}$ Vav-cre mice to resist B16-F10 lung metastasis was reduced, the present study lacks NK cell depletion experiments to confirm that the impaired metastasis control is NK cell-dependent. Therefore, the reduction in antitumor function of NK cells with Hspa9 deletion cannot be definitively concluded. The mechanistic studies will be refined further in future research. Hspa9 deficiency in NK cells was demonstrated to suppress Akt/mTOR signaling. As Hspa9 is pivotal for energy metabolism and anti-apoptotic signaling, cytosolic Hspa9 can inhibit the transcriptional activity of p53, thereby suppressing apoptosis (25). Notably, in cancer contexts, Hspa9 often promotes tumor progression by activating pathways such as PI3K/Akt/mTOR and Wnt/β-catenin (26). The present findings suggest that within NK cells, the loss of Hspa9 negatively impacts activation of the Akt/mTOR pathway.

Long-term Hspa9 deficiency may induce compensatory upregulation of other heat shock proteins (such as Hspa1 and Hspa8) by activating the mitochondrial unfolded protein response and heat shock factor 1 (HSF1) (27). These chaperone proteins help maintain cytosolic protein homeostasis and inhibit apoptotic pathways, thereby alleviating cellular dysfunction caused by Hspa deficiency and modulating the final phenotype. However, the compensatory effect is highly dependent on cell type, stress intensity and duration. Upregulation of Hspa1b and Hspa8b has been observed in certain models, such as Smyd1b mutant zebrafish (28), supporting this compensatory mechanism. Therefore, in future studies, the expression levels of family members including Hspa1 and Hspa8 will be simultaneously monitored to more accurately assess their compensatory contributions.

Targeting Hspa9 in NK cells holds promise but faces notable challenges. To achieve NK cell-specific modulation, two strategies are feasible: i) NK-directed nanoparticles, such as anti-CD56-conjugated lipid nanoparticles delivering small interfering RNA or CRISPR components; and ii) *ex vivo* genetic modification of NK cells followed by adoptive transfer. The nanoparticle approach enables systemic administration but suffers from liver sequestration and limited targeting efficiency. *Ex vivo* modification offers precise control but is complex and costly. Future efforts should prioritize developing specific Hspa9 tools and optimizing delivery vectors using unique NK cell surface markers.

In conclusion, the present study uncovers a critical and previously uncharacterized role for Hspa9 in regulating NK cell function. Hspa9 is essential for maintaining their cytotoxic and cytokine-producing capabilities. Hspa9-deficiency also resulted in suppression of the mTOR/Akt signaling pathway in NK cells. To the best of our knowledge, these findings demonstrate for the first time the role of Hspa9 in regulating NK cell function, broadening the understanding of its function and the regulatory mechanisms of NK cell biology.

Acknowledgements

Not applicable.

Funding

The present work was funded by Guangdong Basic and Applied Basic Research Foundation (grant no. 2022A1515140023, to XZ) and the National Natural Science Foundation of China (grant no. 82201919, to XZ).

Availability of data and materials

The data generated in the present study may be requested from the corresponding author.

Authors' contributions

XZ, JZ and ZW conceptualized the study and designed the experiments and data analysis methods. XZ, JZ, CL and JY conducted all experiments and performed the data analysis. XZ, JZ, JY and ZW prepared the figures, analyzed the data and drafted the manuscript. XZ and ZW confirm the authenticity of all the raw data. All authors have read and approved the final version of the manuscript and agree to be accountable for all aspects of the work.

Ethics approval and consent to participate

The animal experiment protocol was approved by the Animal Ethics Committee of the Sixth Affiliated Hospital of South China University of Technology (Nanhai District People's Hospital of Foshan; approval no. ZXSY-JY-ZXK-250918-002).

Patient consent for publication

Not applicable.

Competing interests

The authors declare that they have no competing interests.

References

1. Mace EM: Human natural killer cells: Form, function, and development. J Allergy Clin Immunol 151: 371-385, 2023.
2. Zhang W, Zhao Z and Li F: Natural killer cell dysfunction in cancer and new strategies to utilize NK cell potential for cancer immunotherapy. Mol Immunol 144: 58-70, 2022.
3. Yan S, Dong J, Qian C, Chen S, Xu Q, Lei H and Wang X: The mTORC1 signaling support cellular metabolism to dictate decidual NK cells function in early pregnancy. Front Immunol 13: 771732, 2022.
4. Cichocki F, Sitnicka E and Bryceson YT: NK cell development and function-plasticity and redundancy unleashed. Semin Immunol 26: 114-126, 2014.
5. Kee BL, Morman RE and Sun M: Transcriptional regulation of natural killer cell development and maturation. Adv Immunol 146: 1-28, 2020.
6. Rawat P and Das A: Differential expression of disparate transcription factor regime holds the key for NK cell development and function modulation. Life Sci 297: 120471, 2022.
7. Ali AK, Nandagopal N and Lee SH: IL-15-PI3K-AKT-mTOR: A critical pathway in the life journey of natural killer cells. Front Immunol 6: 355, 2015.

8. Terrén I, Sandá V, Amarilla-Irusta A, Lopez-Pardo A, Sevilla A, Astarloa-Pando G, Amo L, Zenarruzabeitia O, Scorrano L and Borrego F: IL-12/15/18-induced cell death and mitochondrial dynamics of human NK cells. Front Immunol 14: 1211839, 2023.
9. Yokoyama WM and Riley JK: NK cells and their receptors. Reprod Biomed Online 16: 173-191, 2008.
10. Xia M, Wang B, Wang Z, Zhang X and Wang X: Epigenetic regulation of NK cell-mediated antitumor immunity. Front Immunol 12: 672328, 2021.
11. Zhang R, Wang XX, Xie JF, Yao TT, Guo QW, Wang Q, Ding Z, Zhang JP, Zhang MR and Xu LC: Cypermethrin induces Sertoli cell apoptosis through endoplasmic reticulum-mitochondrial coupling involving IP3R1-GRP75-VDAC1. Reprod Toxicol 124: 108552, 2024.
12. Li X, Zhao X, Qin Z, Li J, Sun B and Liu L: Regulation of calcium homeostasis in endoplasmic reticulum-mitochondria crosstalk: Implications for skeletal muscle atrophy. Cell Commun Signal 23: 17, 2025.
13. Oh SS and Narver HL: Mouse and rat anesthesia and analgesia. Curr Protoc 4: e995, 2024.
14. Zeng X, Dong X, Ma Y and Yao J: Chemokine (C-X-C motif) ligand 1 maintains the immune surveillance function of natural killer cells via the PDK2/mTOR signaling pathway. Cell Biol Toxicol 39: 2227-2241, 2023.
15. Liang C, Song R, Zhang J, Yao J, Guan Z and Zeng X: Melatonin enhances NK cell function in aged mice by increasing T-bet expression via the JAK3-STAT5 signaling pathway. Immun Ageing 21: 59, 2024.
16. He J, Wang Y, Liu T, Liu G, Chen S, Li Q, Quan Y, Yang H, Feng J, Wang S, *et al*: Stage-specific requirement of kinase PDK1 for NK cells development and activation. Cell Death Differ 26: 1918-1928, 2019.
17. Wang M, Chen X, Zhang H, Li L, Xu Y, Lu W and Lu Y: ENSMUST00000147869 regulates proliferation and fibrosis of mesangial cells in diabetic nephropathy by interacting with Hspa9. IUBMB Life 74: 419-432, 2022.
18. Pan F, Gan J, Hu M, Song Y and Wu X: HSPA9/HMGB1 regulates myocardial fibrosis in atrial fibrillation via TGF-β1/Smad pathway and autophagy. Mol Biol Rep 52: 815, 2025.
19. Lu WJ, Lee NP, Kaul SC, Lan F, Poon RT, Wadhwa R and Luk JM: Mortalin-p53 interaction in cancer cells is stress dependent and constitutes a selective target for cancer therapy. Cell Death Differ 18: 1046-1056, 2011.
20. Elwakeel A: Abrogating the interaction between p53 and Mortalin (Grp75/HSPA9/mtHsp70) for cancer therapy: The story so far. Front Cell Dev Biol 10: 879632, 2022.
21. Zhao F, Cui Z, Wang P, Zhao Z, Zhu K, Bai Y, Jin X, Wang L and Lu L: GRP75-dependent mitochondria-ER contacts ensure cell survival during early mouse thymocyte development. Dev Cell 59: 2643-2658.e7, 2024.
22. Craven SE, French D, Ye W, de Sauvage F and Rosenthal A: Loss of Hspa9b in zebrafish recapitulates the ineffective hematopoiesis of the myelodysplastic syndrome. Blood 105: 3528-3534, 2005.
23. Kaul SC, Deocaris CC and Wadhwa R: Three faces of mortalin: A housekeeper, guardian and killer. Exp Gerontol 42: 263-274, 2007.
24. Ferré CA, Thouard A, Bétourné A, Le Dorze AL, Belenguer P, Miquel MC, Peyrin JM, Gonzalez-Dunia D and Szelechowski M: HSPA9/Mortalin mediates axo-protection and modulates mitochondrial dynamics in neurons. Sci Rep 11: 17705, 2021.
25. Wadhwa R, Yaguchi T, Hasan MK, Mitsui Y, Reddel RR and Kaul SC: Hsp70 family member, mot-2/mthsp70/GRP75, binds to the cytoplasmic sequestration domain of the p53 protein. Exp Cell Res 274: 246-253, 2002.
26. Xu M, Jin T, Chen L, Zhang X, Zhu G, Wang Q and Lin Z: Mortalin is a distinct bio-marker and prognostic factor in serous ovarian carcinoma. Gene 696: 63-71, 2019.
27. Ramos E, Romero A, Marco-Contelles J, López-Muñoz F and Del Pino J: Modulation of heat shock response proteins by ASS234, targeted for neurodegenerative diseases therapy. Chem Res Toxicol 31: 839-842, 2018.
28. Xiao H, Li M, Zhong Y, Patel A, Xu R, Zhang C, Athey TW, Fang S, Xu T and Du S: Hsf1 is essential for proteotoxic stress response in smyd1b-deficient embryos and fish survival under heat shock. FASEB J 39: e70283, 2025.